Minimal Microscopic Model for Liquid Polyamorphism and Waterlike Anomalies

Institut Lumière Matière, Université de Lyon, Université Claude Bernard Lyon 1, CNRS, F-69622 Villeurbanne, France

Mikhail A. Anisimov

Department of Chemical and Biomolecular Engineering and Institute for Physical Science and Technology, University of Maryland, College Park, Maryland 20742, USA



(Received 16 June 2021; revised 23 July 2021; accepted 21 September 2021; published 27 October 2021)

Liquid polyamorphism is the intriguing possibility for a single component substance to exist in multiple liquid phases. We propose a minimal model for this phenomenon. Starting with a binary lattice model with critical azeotropy and liquid-liquid demixing, we allow interconversion of the two species, turning the system into a single-component fluid with two states differing in energy and entropy. Unveiling the phase diagram of the noninterconverting binary mixture gives unprecedented insight on the phase behaviors accessible to the interconverting fluid, such as a liquid-liquid transition with a critical point, or a singularity-free scenario, exhibiting thermodynamic anomalies without polyamorphism. The model provides a unified theoretical framework to describe supercooled water and a variety of polyamorphic liquids with waterlike anomalies.

DOI: 10.1103/PhysRevLett.127.185701

The Ising model and the lattice-gas model are landmarks in the history of science. They have provided an explanation of phase transitions based on statistical physics and paved the way to the understanding of universality in critical phenomena, one of the greatest achievements in twentieth century physics. The lattice-gas model, although minimal, with sites on a lattice either occupied or empty, captures the essential physics of all fluids near their liquid-vapor critical point. Here we propose a minimal, two-state model for single-component fluids with waterlike anomalies.

Water is an everyday liquid, but, for the scientist, it is a puzzling material, which concentrates the largest number of anomalies compared to the "ordinary" liquid [1]. One intriguing theoretical explanation of these anomalies is "liquid polyamorphism" (LP) [2], which posits that water may exist under two distinct liquid phases at low temperature. Observing this liquid-liquid transition (LLT) is challenging, because at the required conditions ice is the stable phase, and the liquid phase has a very short lifetime. Nevertheless, a recent study has reported observation of the two liquid phases of water [3]. In addition to the quantum case of superfluidity in helium isotopes, LP has also been reported in experiments on phosphorus [4], hydrogen [5], and recently sulfur [6]. Notwithstanding, LP, in contrast to well-known crystal polymorphism, is still viewed as an exotic and controversial phenomenon. Some atomistic models with a soft repulsion potential demonstrate the possibility of LLT in a pure substance [7–9]. A generic, but more phenomenological approach attributes this phenomenon to equilibrium interconversion of two alternative molecular or supramolecular structures [10]. Conceptually, this approach resonates with the idea of two competing local structures in cold and supercooled water [11].

An equation of state (EOS) based on interconversion of alternative states incorporating a LLT was successfully used to describe the phase behavior and thermodynamic anomalies in two simulated atomistic models of water, ST2 [12] and TIP4P/2005 [13,14] or its charge-scaled versions [15]. A similar EOS was also used to correlate the experimental thermodynamic properties of supercooled water [16,17] and hydrogen [18]. Another two-state EOS without a LLT was able to reproduce simulation results for a monatomic water model which does not show LP [19]. However, two-state phenomenology still lacks a clear connection with the microscopic nature of underlying intermolecular interactions. In this work, we mend this gap with a minimalistic lattice model. Previous lattice models [20–24] were able to produce waterlike anomalies, but they were focused on the one-component fluid. Simulations can explore families of model interaction potentials with waterlike anomalies by varying a parameter [15,25–28], but they are intrinsically confined to the one-component fluid. Here, we go one step back to first display the case when interconversion is absent, making the system a binary fluid. This gives a phase diagram in three dimensions: temperature T, pressure P, and fraction x of one of the components. Then, we turn interconversion on, which makes x a function of T and P, dictated by interconversion equilibrium conditions. The system becomes a one-component fluid, whose phase diagram can be thought as a 2D-manifold immersed in the underlying 3D binary phase diagram. This gives unprecedented insight on the way liquid-liquid polyamorphism may emerge, and

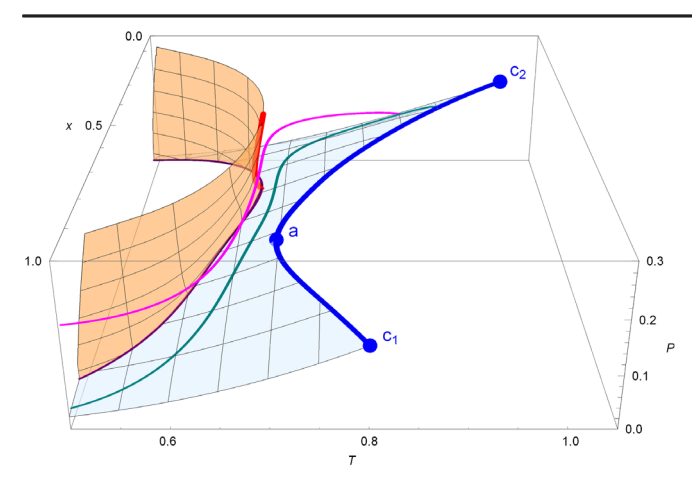


FIG. 1. T-P-x phase diagram of a binary mixture with $\omega_1=1.6$, $\omega_2=2$, and $\omega_{12}=1.04$. The light blue surface shows the liquid in equilibrium with its vapor, terminating at the liquid-vapor critical line (dark blue) which reaches its minimum at the critical azeotrope **a**. The liquid-vapor critical points of the pure components are designated as \mathbf{c}_1 and \mathbf{c}_2 . The orange surface shows the liquid-liquid equilibrium, terminating at the LLcl (red). The two surfaces intersect along a triple line (purple) where two liquids and one vapor coexist. The metastable parts of the liquid-liquid equilibrium surface and critical line are omitted for clarity. When the two species interconvert, the fraction x becomes a function of temperature and pressure, shown as curves for the liquid-vapor (cyan) and the P=0.18 isobar (magenta) for e=3 and s=4.

provides a general theoretical framework for understanding the variety of possible cases, e.g., with or without LLT, and with opposite signs of the LLT dP/dT slopes, such as water and sulfur.

Binary mixture without interconversion of species.—In order to understand the various scenarios that can be obtained for the interconverting fluid, a prerequisite is the knowledge of the underlying phase diagram for the noninterconverting, binary mixture. We use the classic compressible binary mixture on a lattice [29–31] (see also Supplemental Material [32]). Consider a lattice whose sites can be either empty or occupied by only one particle of two species 1 and 2. The empty sites do not interact with the rest, whereas particles interact with their z nearest neighbors, with an interaction energy $-2\omega_1/z$, $-2\omega_2/z$, and $-2\omega_{12}/z$, for 1-1, 2-2, and 1-2 pairs, respectively. Figure 1 shows the T - P - x phase diagram for a generic case, with $\omega_1 = 1.6$, $\omega_2 = 2$, and $\omega_{12} = 1.04$. At low temperature, liquid-liquid demixing occurs, with a liquid-liquid critical line (LLcl). This diagram belongs to an unusual case of type II critical behavior in the classification of Konynenburg and Scott [35], with in addition a reentrant cusp in the P-T projection of the critical line, making this case special [36]. T - P, T - x, and $T - \rho$ projections, where ρ is the density, are displayed in Fig. S1 [32], together with those for the symmetric ($\omega_1 = \omega_2 = 2$, $\omega_{12} = 1.24$) and tricritical ($\omega_1 = 1.6, \ \omega_2 = 2, \ \omega_{12} = 1$) cases. Fig. S2 [32] shows the T - P - x phase diagram of the latter.

One-component system with interconversion between states.—To introduce LP, we allow the two species 1 and 2 to interconvert. In a binary system, the two chemical potentials for each pure species are independent, which means that adding a constant to one of them does not change the phase diagram nor thermodynamic properties. In contrast, with interconversion, the difference between the chemical potentials is restricted by the reaction equilibrium condition that depends on T and P. We introduce this through the changes in energy e and in entropy s, when a particle changes state from 1 to 2 [32]. This could, for instance, correspond to internal degrees of freedom which are frozen in state 1, but become accessible in state 2, which causes the number of internal configurations and hence the entropy in 2 to be higher than in 1. In the case of water, the model can be thought as a coarse grain model where a "particle" is a group of water molecules, who could be tetrahedrally arranged (state 1 with a lower energy and entropy) or more disordered (state 2 with a higher energy and entropy). This is reminiscent of the A and B states [10] or ρ and ψ structures [37] in phenomenological models proposed for water. We note that as we do not need to specify the origin of the energy and entropy differences, our model is generic and can be applied to any type of polyamorphic fluid.

With interconversion, the system effectively becomes a single-component one, which follows specific x(T, P)paths. Two examples are given in Fig. 1. The first path shows liquid-vapor equilibrium in the interconverting fluid. The fraction x decreases with increasing temperature, until a single liquid-vapor critical point is reached; it is located on the liquid-vapor critical line of the underlying binary phase diagram. The second path in Fig. 1 shows how the fraction changes with temperature in the interconverting fluid, along an isobar in the liquid region. For that particular choice (P = 0.18), the path passes very close to the LLcl of the underlying binary phase diagram, but without crossing the liquid-liquid equilibrium surface. By tuning the model parameters, this crossing can be obtained for a range of pressures or avoided, either generating LP [e.g., a LLT with a liquid-liquid critical point (LLCP)] in the interconverting fluid, or not.

Figure 2 shows the various possible scenarios obtained by varying the nonideal mixing parameter ω_{12} , while keeping all other parameters constant ($\omega_1 = 1.6$, $\omega_2 = 2$, e = 3 and s = 4). For $\omega_{12} > 1.15$, there is only one liquid, with a liquid-vapor transition. The absence of a LLT is rigorously proven by studying the spinodal curves, whose temperature admits an analytic expression as a function of x [32]. The spinodals are physically acceptable only if they are located at densities below 1, the maximum possible value for the model when all sites are occupied. For $\omega_{12} > 1.15$, only the liquid-vapor spinodals are acceptable.

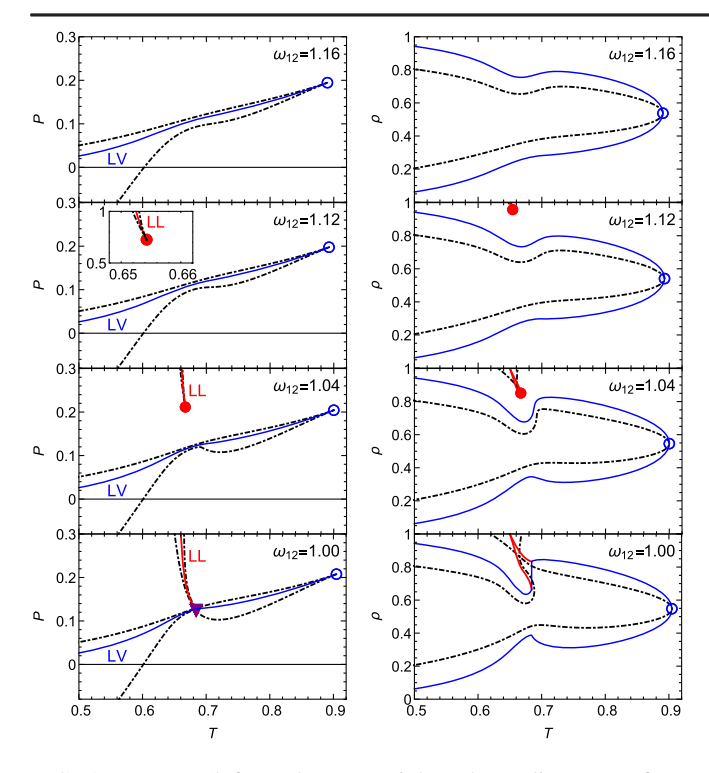


FIG. 2. T-P (left) and $T-\rho$ (right) phase diagrams of an interconverting fluid, for $\omega_1=1.6$, $\omega_2=2$, illustrating the four possible scenarios: singularity free ($\omega_{12}=1.16$), second critical point with monotonic spinodal ($\omega_{12}=1.04$), critical-point free ($\omega_{12}=1$). Curves shown are liquid-vapor [(LV), solid blue] and liquid-liquid [(LL), solid red] equilibria; spinodals (dash-dotted black). Empty blue circle: LV critical point; filled red circle: LL critical point; purple triangle: triple point. The inset for $\omega_{12}=1.12$ shows the LLT occurring at higher pressure than displayed in the main graph.

This case, with no LLT, corresponds to the singularity-free (SF) scenario [20]. Figure 2 (top) illustrates this case for $\omega_{12} = 1.16$: along the liquid-vapor equilibrium, the pressure is monotonic, whereas the density is not. This is the most prominent waterlike anomaly, which is found for all cases shown in Fig. 2. When ω_{12} is lowered below 1.15, a LLT appears, terminating in a LLCP. Three distinct cases are found. For $1.15 > \omega_{12} > 1.1075$, the LLCP is at relatively high pressure, and the liquid-vapor spinodal pressure is a monotonically increasing function of temperature; this corresponds to the "second critical point scenario" [38]. For $1.1075 > \omega_{12} > 1.018$, there is still a first-order LLT terminating in a LLCP, but the liquid-vapor spinodal pressure exhibits a maximum and a minimum as a function of temperature; this is a possibility that, to our knowledge, had not been proposed yet. Finally, for ω_{12} < 1.018, there is a LLT, but the LLCP disappears because it lies beyond the spinodal; this corresponds to the critical point free scenario [39,40]. In this last case, there is a triple point where two liquids and vapor coexist. Figure 3 shows how the metastable continuations of the LLT and the

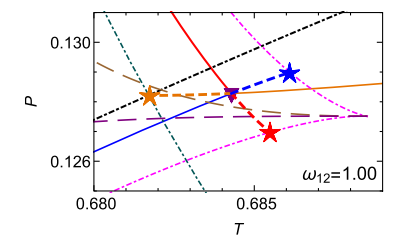


FIG. 3. Close-up in the T-P plane for the case $\omega_{12} = 1$ displayed in Fig. 2. The spinodals (dot-dashed curves) have been colored for clarity, as well as the three two-phase equilibrium lines (solid curves), whose metastable continuation is shown with short dashed curves. Their intersections with the spinodals define three "Speedy points" (stars). Two lines of anomalies (long-dashed) are also shown, see text and Fig. 4 for details.

two liquid-vapor transitions each end when they touch the corresponding spinodal. The metastable equilibrium ceases because one of the phase becomes unstable. Our microscopic model thus confirms the findings of Ref. [41], based on a phenomenological EOS, that a spinodal does not necessarily intersect a binodal at a critical point, but may terminate it at a so-called "Speedy point." This settles a 20-year old controversy [42–44] and demonstrates the viability of the critical-point free scenario.

Lines of extrema of thermodynamic properties.—The vast majority of liquids shows a monotonic increase of molar volume, isothermal compressibility κ_T , and isobaric heat capacity C_P when temperature increases along isobars. A liquid is anomalous when it exhibits extrema in these quantities, and water is considered to be the most anomalous liquid [1]: along isobars, stable water shows maxima of ρ and minima of κ_T , and maxima of κ_T have been reported in metastable water [45,46]. Our model captures such anomalies in the interconverting fluid, and Fig. 4 shows their loci for each of the four cases displayed in Fig. 2. The behavior of x, ρ , and κ_T in the four cases along the same isobar at P = 0.18 is given in Fig. S3 [32]. The extrema lines follow a familiar pattern, obeying thermodynamic rules: when the lines of ρ and κ_T extrema along isobars intersect, the former reaches an extremum temperature [20], and when the lines of ρ extrema along isobars and C_P extrema along isotherms intersect, the former reaches an extremum pressure [47]. As shown in Fig. 1, the anomalies observed in the interconverting fluid are related to the liquid-liquid equilibrium and critical line in the underlying binary fluid, whose distances to the T-xpath followed with interconversion varies with P and ω_{12} . The cases $\omega_{12} = 1.16$ and 1.12 are similar, with the loci of extrema avoiding the liquid-vapor spinodal which thus keeps a monotonic pressure [48]. For $\omega_{12} = 1.12$, Fig. S4 shows a close-up near the spinodal, and Fig. S5 provides an enlarged view emphasizing the similarity with the lines of anomalies for real water [32]. In the cases with a LLCP, $\omega_{12} = 1.12$ and 1.04, lines of κ_T maxima along isobars and of C_P maxima along isotherms emanate from the LLCP.

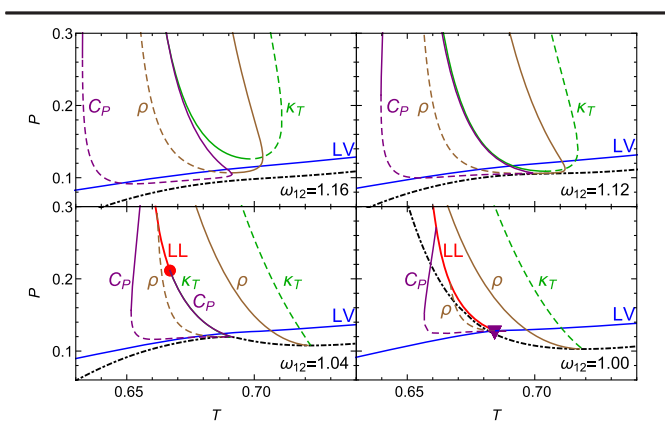


FIG. 4. Lines of extrema in the T-P plane for the four cases displayed in Fig. 2. Solid and dashed curves show maxima and minima, respectively, of density (ρ , brown) and isothermal compressibility (κ_T , green) along isobars, and of isobaric heat capacity (C_P , purple) along isotherms. Also shown are the liquid-vapor equilibrium (LV, solid blue curve), the high density liquid spinodal (dot-dashed black curve), the LLCP (red disc), and the liquid-liquid-vapor triple point (purple triangle).

In the case $\omega_{12}=1.04$, the extrema in ρ , κ_T , and C_P eventually intersect the liquid-vapor spinodal, causing it to go through extremum pressures [48] (see Fig. S6 [32] for a close-up near the maximum spinodal pressure). In the case $\omega_{12}=1$, the LLCP is pushed away in the unstable region. The line of maxima in κ_T along isobars has disappeared; instead, κ_T in the liquid metastable below the LLT diverges at the low temperature liquid-liquid spinodal. Figure 3 shows how the lines of minima in ρ along isobars and in C_P along isotherms extend into the metastable low-density liquid region, until simultaneously reaching its maximum temperature. There is now a continuous line of instability bounding the high-density liquid region at low pressure and at low temperature (Fig. 4), just as hypothesized by Speedy in 1982 [48].

Discussion.—Thermodynamics of LP has been mostly treated at the phenomenological level, based on an *ad hoc* free energy specified with a modified van der Waals EOS [39,41] or with mixing terms (two-state models) [10,11]. Attempts based on statistical mechanics to derive the free energy from a microscopic cell model exist [20–24,49]. However, to generate the density maximum of water, they all introduce "by hand" a "local" density difference between the two states. Each cell changed occupancy [22] or volume [20,23,24] according to its actual state. Similarly, statistical mechanics and simulation approaches introduce two length scales [7–9,25,50–53] to describe waterlike anomalies and LP, suggesting that the presence of two length scales is a ubiquitous ingredient for such phenomena.

These aspects have been a long-standing source of criticism against the application of two-state models to water, because the supposed large density contrast between the two states (e.g., 24% [22] or 38% [24]) would be easily

detected in x-ray or neutron scattering experiments [54]. Our microscopic two-state model settles this debate. While generating the density anomaly and the possibility of LP, it does not require two different length scales: it is a fixed lattice in which each site can be occupied by only one particle without an explicit length or volume difference. We found that even in the perfectly symmetric case $\omega_1 = \omega_2$, for which the pure fluids under the same conditions would have exactly the same density, appropriate choices of e and s lead to waterlike anomalies in the interconverting fluid. This underlines that nonideality in the mixture is the primary ingredient for anomalous behavior. This can be understood with Fig. S1 (top row) [32]: for instance, the path followed by x as a function of temperature in the interconverting fluid can be tuned to cross the LLcl at a given pressure, thus generating the second critical point scenario and the associated anomalies. Even in the SF scenario without a LLT, the path followed by x along liquid-vapor equilibrium can be tuned to pass close to the azeotrope a, before reaching the liquid-vapor critical line at higher temperature and higher density, which generates a nonmonotonic density. In the more general case where $\omega_1 \neq \omega_2$ (Fig. S1, middle row [32]), the hypothetical pure fluids 1 and 2 have different densities under the same conditions of temperature and pressure; this further contributes to the density anomaly. This connects to purely phenomenological two-state models such as in Ref. [10], which specify differences between the hypothetical pure fluids 1 or 2, but do not imply a local density contrast in the interconverting fluid, i.e., bimodality of the distribution of local particle volumes. This resolves the controversy around the interpretation of two-state models: for instance, the "locally favored structure" of Ref. [11] which has "more specific volume than the normal-liquid structure" should be understood as the average structure of the hypothetical pure component, rather than a local lowdensity structure in the interconverting fluid.

In the case of water, it has been argued that the SF scenario could be obtained only in "the artificial limit in which a molecule's hydrogen-bonding connectivity is completely uncorrelated" [46]. This is indeed the case for a cell model studied by Stokely et al. [23] (where the SF scenario is obtained only for zero cooperativity between molecules forming hydrogen bonds), or in the phenomenological model of Ref. [10] (where the SF scenario requires ideal mixing between the two states, $\omega = \omega_1 + \omega_2 - 2\omega_{12} = 0$). Here, we find that, even with significant nonideality in the interactions between the interconverting species, there could be a case with no LLT, corresponding to the SF scenario. Indeed, the LLT exists for large enough ω , but as ω is lowered (i.e., ω_{12}) increased), the LLCP, while staying at finite temperature, moves to higher density, until it reaches inaccessible states with density above 1 (Fig. 2). More generally, depending on the details of the system, it is possible, with physically acceptable parameters and the presence of thermodynamic anomalies, that the LLT occurs in inaccessible regions of the phase diagram (e.g., in the nonthermodynamic habitat [55] at which the metastable liquid has not enough time to equilibrate before crystallization occurs); such a case would be equivalent to the SF scenario. This might also solve the controversy about the existence of a LLT for the TIP4P/ 2005 water potential. Versions with reduced partial charges clearly show a LLT with LLCP [15]. Simulations with the original TIP4P/2005 show critical-like behavior (at temperature above the putative LLCP) consistent with 3D Ising universality class [56], while advanced sampling techniques below the predicted LLCP temperature find an energy landscape with only one liquid phase [57]. This could correspond to the interconverting fluid approaching closely the LLcl without crossing it. Importantly, we show that, for a given fluid, neither the shape of the line of density maxima, nor that of the liquid spinodal limit, nor the existence of κ_T or C_P maxima, is sufficient to identify which scenario is valid: a turning point in the line of density maxima, a monotonic liquid spinodal, or a line of κ_T maxima along isobars, are found in cases with a LLT, as well as in cases without it.

The simplest case we considered, with fixed energy and entropy of interconversion, e and s, already captures all scenarios proposed for water. Other fluids may exhibit different behaviors, such as a LLT with a positive dP/dT slope as found for sulfur [6], or terminated by two (lower and upper) LLCPs; this could be addressed using appropriate functions for e and s. The interconverting lattice fluid thus provides a versatile tool to unify all types of anomalous fluids, with or without liquid polyamorphism.

M. A. A. acknowledges the financial support of the National Science Foundation, Grant No. 1856479, and F. C. that of Agence Nationale de la Recherche, Grant No. ANR-19-CE30-0035-01.

- frederic.caupin@univ-lyon1.fr
- [1] P. Gallo, K. Amann-Winkel, C. A. Angell, M. A. Anisimov, F. Caupin, C. Chakravarty, E. Lascaris, T. Loerting, A. Z. Panagiotopoulos, J. Russo, J. A. Sellberg, H. E. Stanley, H. Tanaka, C. Vega, L. Xu, and L. G. M. Pettersson, Water: A tale of two liquids, Chem. Rev. **116**, 7463 (2016).
- [2] H. E. Stanley, *Liquid Polymorphism* (John Wiley & Sons, New York, 2013), http://dx.doi.org/10.1002/9781 118540350.
- [3] K. H. Kim, K. Amann-Winkel, N. Giovambattista, A. Späh, F. Perakis, H. Pathak, M. L. Parada, C. Yang, D. Mariedahl, T. Eklund, T. J. Lane, S. You, S. Jeong, M. Weston, J. H. Lee, I. Eom, M. Kim, J. Park, S. H. Chun, P. H. Poole, and A. Nilsson, Experimental observation of the liquid-liquid transition in bulk supercooled water under pressure, Science 370, 978 (2020).
- [4] Y. Katayama, Macroscopic separation of dense fluid phase and liquid phase of phosphorus, Science **306**, 848 (2004).

- [5] M. D. Knudson, M. P. Desjarlais, A. Becker, R. W. Lemke, K. R. Cochrane, M. E. Savage, D. E. Bliss, T. R. Mattsson, and R. Redmer, Direct observation of an abrupt insulator-tometal transition in dense liquid deuterium, Science 348, 1455 (2015).
- [6] L. Henry, M. Mezouar, G. Garbarino, D. Sifré, G. Weck, and F. Datchi, Liquid-liquid transition and critical point in sulfur, Nature (London) 584, 382 (2020).
- [7] L. Xu, P. Kumar, S. V. Buldyrev, S. H. Chen, P. H. Poole, F. Sciortino, and H. E. Stanley, Relation between the Widom line and the dynamic crossover in systems with a liquid– liquid phase transition, Proc. Natl. Acad. Sci. U.S.A. 102, 16558 (2005).
- [8] P. Vilaseca and G. Franzese, Isotropic soft-core potentials with two characteristic length scales and anomalous behaviour, J. Non-Cryst. Solids 357, 419 (2011).
- [9] L. Pinheiro, A. Furlan, L. Krott, A. Diehl, and M. Barbosa, Critical points, phase transitions and water-like anomalies for an isotropic two length scale potential with increasing attractive well, Physica A (Amsterdam) 468A, 866 (2017).
- [10] M. A. Anisimov, M. Duška, F. Caupin, L. E. Amrhein, A. Rosenbaum, and R. J. Sadus, Thermodynamics of Fluid Polyamorphism, Phys. Rev. X 8, 011004 (2018).
- [11] H. Tanaka, Simple physical model of liquid water, J. Chem. Phys. **112**, 799 (2000).
- [12] V. Holten, J. C. Palmer, P. H. Poole, P. G. Debenedetti, and M. A. Anisimov, Two-state thermodynamics of the ST2 model for supercooled water, J. Chem. Phys. 140, 104502 (2014).
- [13] R. S. Singh, J. W. Biddle, P. G. Debenedetti, and M. A. Anisimov, Two-state thermodynamics and the possibility of a liquid-liquid phase transition in supercooled TIP₄P/2005 water, J. Chem. Phys. 144, 144504 (2016).
- [14] J. W. Biddle, R. S. Singh, E. M. Sparano, F. Ricci, M. A. González, C. Valeriani, J. L. F. Abascal, P. G. Debenedetti, M. A. Anisimov, and F. Caupin, Twostructure thermodynamics for the TIP4P/2005 model of water covering supercooled and deeply stretched regions, J. Chem. Phys. 146, 034502 (2017).
- [15] R. Horstmann and M. Vogel, Relations between thermodynamics, structures, and dynamics for modified water models in their supercooled regimes, J. Chem. Phys. 154, 054502 (2021).
- [16] F. Caupin and M. A. Anisimov, Thermodynamics of supercooled and stretched water: Unifying two-structure description and liquid-vapor spinodal, J. Chem. Phys. 151, 034503 (2019).
- [17] M. Duška, Water above the spinodal, J. Chem. Phys. 152, 174501 (2020).
- [18] B. Cheng, G. Mazzola, C. J. Pickard, and M. Ceriotti, Evidence for supercritical behaviour of high-pressure liquid hydrogen, Nature (London) **585**, 217 (2020).
- [19] V. Holten, D. T. Limmer, V. Molinero, and M. A. Anisimov, Nature of the anomalies in the supercooled liquid state of the mW model of water, J. Chem. Phys. 138, 174501 (2013).
- [20] S. Sastry, P. G. Debenedetti, F. Sciortino, and H. E. Stanley, Singularity-free interpretation of the thermodynamics of supercooled water, Phys. Rev. E 53, 6144 (1996).
- [21] J. Hrubý and V. Holten, A two-structure model of thermodynamic properties and surface tension of supercooled

- water, in *Proceedings of the 14th International Conference* on the *Properties of Water and Steam, Kyoto, Japan* (Maruzen Co., Ltd, Tokyo, 2004), Vol. 29, pp. 241–246.
- [22] A. Ciach, W. Góźdź, and A. Perera, Simple three-state lattice model for liquid water, Phys. Rev. E 78, 021203 (2008).
- [23] K. Stokely, M. G. Mazza, H. E. Stanley, and G. Franzese, Effect of hydrogen bond cooperativity on the behavior of water, Proc. Natl. Acad. Sci. U.S.A. 107, 1301 (2010).
- [24] C. A. Cerdeiriña, J. Troncoso, D. González-Salgado, P. G. Debenedetti, and H. E. Stanley, Water's twocritical-point scenario in the Ising paradigm, J. Chem. Phys. 150, 244509 (2019).
- [25] H. M. Gibson and N. B. Wilding, Metastable liquid-liquid coexistence and density anomalies in a core-softened fluid, Phys. Rev. E 73, 061507 (2006).
- [26] F. Smallenburg and F. Sciortino, Tuning the Liquid-Liquid Transition by Modulating the Hydrogen-Bond Angular Flexibility in a Model for Water, Phys. Rev. Lett. 115, 015701 (2015).
- [27] D. Dhabal, C. Chakravarty, V. Molinero, and H. K. Kashyap, Comparison of liquid-state anomalies in Stillinger-Weber models of water, silicon, and germanium, J. Chem. Phys. 145, 214502 (2016).
- [28] J. Russo, K. Akahane, and H. Tanaka, Water-like anomalies as a function of tetrahedrality, Proc. Natl. Acad. Sci. U.S.A. 115, E3333 (2018).
- [29] N. Trappeniers, J. Schouten, and C. Ten Seldam, Gas-gas equilibrium and the two-component lattice-gas model, Chem. Phys. Lett. **5**, 541 (1970).
- [30] J. Schouten, C. Ten Seldam, and N. Trappeniers, The two-component lattice-gas model, Physica (Utrecht) 73, 556 (1974).
- [31] D. Furman, S. Dattagupta, and R. B. Griffiths, Global phase diagram for a three-component model, Phys. Rev. B 15, 441 (1977).
- [32] See Supplemental Material http://link.aps.org/supplemental/ 10.1103/PhysRevLett.127.185701 which includes Refs. [33,34], for additional figures and details about thermodynamic calculations for the binary mixture and the case with interconversion.
- [33] N. Trappeniers and J. Schouten, Gas-gas equilibrium in the system neon-krypton, Phys. Lett. 27A, 340 (1968).
- [34] J. S. Rowlinson and F. L. Swinton, *Liquids and Liquid Mixtures*, 3rd ed. (Butterworth-Heinemann, London, 1982), https://doi.org/10.1016/C2013-0-04175-8.
- [35] P. H. van Konynenburg and R. L. Scott, Critical lines and phase equilibria in binary van der Waals mixtures, Phil. Trans. R. Soc. A 298, 495 (1980).
- [36] A. Van Pelt, Critical phenomena in binary fluid mixtures: Classification of phase equilibria with the simplified-perturbed-hard-chain theory, Ph.D. thesis, TU Delft, Delft, Netherlands, 1992.
- [37] H. Tanaka, Liquid-liquid transition and polyamorphism, J. Chem. Phys. 153, 130901 (2020).
- [38] P. H. Poole, F. Sciortino, U. Essmann, and H. E. Stanley, Phase behaviour of metastable water, Nature (London) **360**, 324 (1992).

- [39] P. H. Poole, F. Sciortino, T. Grande, H. E. Stanley, and C. A. Angell, Effect of Hydrogen Bonds on the Thermodynamic Behavior of Liquid Water, Phys. Rev. Lett. **73**, 1632 (1994).
- [40] C. A. Angell, Insights into phases of liquid water from study of its unusual glass-forming properties, Science **319**, 582 (2008).
- [41] P. Chitnelawong, F. Sciortino, and P. H. Poole, The stability-limit conjecture revisited, J. Chem. Phys. 150, 234502 (2019).
- [42] P.G. Debenedetti, Supercooled and glassy water, J. Phys. Condens. Matter **15**, R1669 (2003).
- [43] R. J. Speedy, Supercooled and glassy water, J. Phys. Condens. Matter 16, 6811 (2004).
- [44] P. G. Debenedetti, Reply to Comment on Supercooled and glassy water, J. Phys. Condens. Matter 16, 6815 (2004).
- [45] V. Holten, C. Qiu, E. Guillerm, M. Wilke, J. Rička, M. Frenz, and F. Caupin, Compressibility anomalies in stretched water and their interplay with density anomalies, J. Phys. Chem. Lett. 8, 5519 (2017).
- [46] K. H. Kim, A. Späh, H. Pathak, F. Perakis, D. Mariedahl, K. Amann-Winkel, J. A. Sellberg, J. H. Lee, S. Kim, J. Park, K. H. Nam, T. Katayama, and A. Nilsson, Maxima in the thermodynamic response and correlation functions of deeply supercooled water, Science 358, 1589 (2017).
- [47] P. H. Poole, I. Saika-Voivod, and F. Sciortino, Density minimum and liquid–liquid phase transition, J. Phys. Condens. Matter 17, L431 (2005).
- [48] R. J. Speedy, Stability-limit conjecture. An interpretation of the properties of water, J. Phys. Chem. 86, 982 (1982).
- [49] G. Franzese, M. I. Marqués, and H. E. Stanley, Intramolecular coupling as a mechanism for a liquid-liquid phase transition, Phys. Rev. E 67, 011103 (2003).
- [50] T. M. Truskett, P. G. Debenedetti, S. Sastry, and S. Torquato, A single-bond approach to orientationdependent interactions and its implications for liquid water, J. Chem. Phys. 111, 2647 (1999).
- [51] A. B. de Oliveira, P. A. Netz, and M. C. Barbosa, An ubiquitous mechanism for water-like anomalies, Europhys. Lett. **85**, 36001 (2009).
- [52] T. Urbic, Modelling water with simple Mercedes-Benz models, Mol. Simul. 45, 279 (2019).
- [53] A. P. Bartók, G. Hantal, and L. B. Pártay, Insight into Liquid Polymorphism from the Complex Phase Behavior of a Simple Model, Phys. Rev. Lett. 127, 015701 (2021).
- [54] G. N. I. Clark, G. L. Hura, J. Teixeira, A. K. Soper, and T. Head-Gordon, Small-angle scattering and the structure of ambient liquid water, Proc. Natl. Acad. Sci. U.S.A. 107, 14003 (2010).
- [55] S. B. Kiselev and J. F. Ely, Parametric crossover model and physical limit of stability in supercooled water, J. Chem. Phys. 116, 5657 (2002).
- [56] P. G. Debenedetti, F. Sciortino, and G. H. Zerze, Second critical point in two realistic models of water, Science **369**, 289 (2020).
- [57] A. Jedrecy, A. M. Saitta, and F. Pietrucci, Free energy calculations and unbiased dynamics reveal a continuous liquid-liquid transition in water no man's land, arXiv: 2106.08263.